

Staged cooling of a fusion-grade plasma in a tokamak thermal quench

Jun Li

*Theoretical Division, Los Alamos National Laboratory, Los Alamos, New Mexico 87545, USA and
School of Nuclear Science and Technology, University of Science and Technology of China, Hefei, Anhui 230026, China*

Yanzeng Zhang and Xian-Zhu Tang

Theoretical Division, Los Alamos National Laboratory, Los Alamos, New Mexico 87545, USA

In tokamak disruptions where the magnetic connection length becomes comparable to or even shorter than the plasma mean-free-path, parallel transport can dominate the energy loss and the thermal quench of the core plasma goes through four phases (stages) that have distinct temperature ranges and durations. The main temperature drop occurs while the core plasma remains nearly collisionless, with the parallel electron temperature $T_{e\parallel}$ dropping in time t as $T_{e\parallel} \propto t^{-2}$ and a cooling time that scales with the ion sound wave transit time over the length of the open magnetic field line. These surprising physics scalings are the result of effective suppression of parallel electron thermal conduction in an otherwise bounded collisionless plasma, which is fundamentally different from what are known to date on electron thermal conduction along the magnetic field in a nearly collisionless plasma.

I. INTRODUCTION

The energy confinement time of a fusion-grade plasma in an ITER-like tokamak reactor is around 1 second (s). [1] This is set by plasma transport across magnetic field lines, or more accurately, nested magnetic surfaces. [2] When a major disruption occurs, such a plasma is expected to lose most of its thermal energy over a period of around 1 millisecond (ms) or so, as noted in the original ITER design document. [3] A dedicated experimental campaign on JET [4], after the initial ITER design was completed [5], revealed that the thermal quench (TQ) duration could vary greatly, from 0.05 to 3.0 ms. The significance of a tokamak thermal quench is that it marks the point of no return in a tokamak disruption. It not only brings a thermal load management issue at the divertor plates and first wall, but also determines the runaway seeding for the subsequent current quench as well as the parallel electric field that could drive avalanche growth of runaway electrons. Since the faster a thermal quench is, the more problematic it becomes for effective mitigation, there are practical interests and urgencies in understanding the fundamentals of the transport physics that are responsible for the rapid thermal quench, particularly the large variation in its duration.

The 3-4 order of magnitude faster plasma energy loss rate in a tokamak disruption [4, 6, 7] is intuitively understood as the result of parallel transport along open magnetic field lines dominating over the perpendicular transport, which is across the magnetic field lines. For that to materialize, the magnetic field lines must connect the hot fusion plasma of 10-15 KeV temperature directly to a cold and dense plasma, which would also serve as a radiative energy sink. This is known to occur in at least two scenarios. The first and more common one of the naturally occurring disruptions has the globally stochastic magnetic field lines connecting the hot core plasma directly onto the divertor surface and/or the first wall, as the result of large-scale magnetohydrodynamic instabilities destroying nested magnetic surfaces. [8-11] The other is high-Z impurity injection in the form of deliberately injected solid pellets or accidentally falling tungsten debris. [12-15] In both sit-

uations, a nearly collisionless plasma is made to intercept a radiative cooling mass, being that an ablated pellet or a vapor-shielded wall.

The simplest problem setup to decipher the parallel cooling physics is to unwind the open field lines into a slab and have a hot plasma of temperature T_0 bounded by thermobath boundary at the two ends that recycles plasma particles to clamp the temperature of the recycled plasma particles to $T_w \ll T_0$. The length of the slab or field line, $x \in [-L_B, L_B]$, is twice the magnetic connection length L_B . The other characteristic length of the problem is the parallel mean-free-path λ_{mfp} , which is tens of kilometers for a plasma of $T_0 = 10-15$ KeV and $n_e = 10^{19-20} \text{m}^{-3}$. The ratio of the two is the Knudsen number $K_n \equiv \lambda_{mfp}/L_B$, and it sets the different cooling regimes (stages) that a thermal quench can go through. For an initial plasma of $K_n \geq 1$, the TQ would start with the (nearly) collisionless phase (regime) and eventually transition to the collisional phase after the plasma cools down sufficiently as $K_n \propto T_e^2/n_e$. [16-19] The simplicity of this prototypical problem setup reinforces the general importance and broad applicability of the underlying plasma cooling physics in fusion as well as non-fusion applications, which will be shown in this paper to present a number of surprises.

The prevailing view on plasma thermal quench is the dominant role of electron *parallel thermal conduction*. This is described in the collisional limit by Braginskii closure for parallel electron conduction flux [20]

$$q_{e\parallel} \equiv \int m_e \tilde{\mathbf{v}}^2 \tilde{v}_{\parallel} f_e d^3\mathbf{v} = -3.16 \frac{n_e T_e \tau_e}{m_e} \frac{\partial T_e}{\partial x} \sim n_e v_{th,e} T_e \frac{\lambda_{mfp}}{L_B}, \quad (1)$$

with τ_e the electron collision time, m_e the electron mass, $v_{th,e} = \sqrt{T_e/m_e}$ the electron thermal speed, and $\tilde{\mathbf{v}} = \mathbf{v} - \mathbf{V}_e$ the peculiar velocity. As the collisionality reduces, $q_{e\parallel}$ scales up linearly with K_n , $q_{e\parallel} \propto K_n$. This would start to break down when K_n gets above 10^{-2} or so, and when $K_n \sim 1$ or $K_n \gg 1$, $q_{e\parallel}$ would *retain the $n_e v_{th,e} T_e$ scaling* but the K_n term

is replaced by a saturated numerical factor $\alpha \sim 0.1$, [17]

$$q_{e\parallel} = \alpha n_e v_{th,e} T_e. \quad (2)$$

With the so-called flux-limiting form of Eq. (2) in the collisionless or free-streaming regime [21], one finds the solution of the heat conduction equation in the bounded domain of $x \in [-L_B, L_B]$ showing a thermal quench duration

$$\tau_{TQ} \sim L_B / v_{th,e}. \quad (3)$$

This suggests a very fast thermal quench indeed, on the order of the thermal electron ma over the open magnetic field line, for a tokamak plasma having $K_n \sim 1$ or $K_n \gg 1$ at the onset of a disruption.

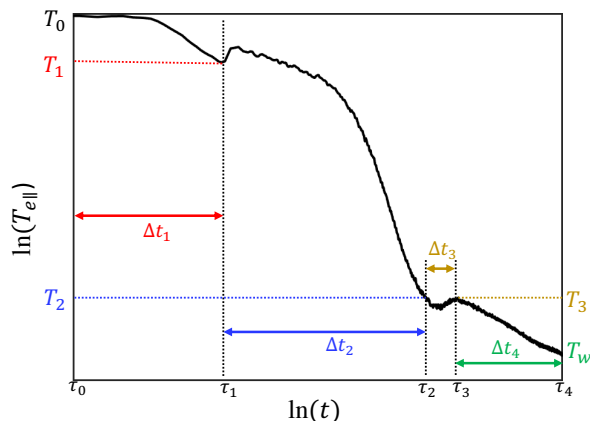


FIG. 1: Schematic view of core $T_{e\parallel}$ evolution in log-log scale from VPIC simulations corresponding to Fig. 2.

Here we show that the core plasma cooling in a bounded plasma like that of a tokamak disruption follows *qualitatively and quantitatively different* behaviors. Specifically the parallel electron temperature $T_{e\parallel}(x=0, t)$ goes through four distinct stages with durations $\Delta t_{1,2,3,4}$ segmented by transition temperatures of $T_{1,2,3}$, as illustrated in Fig. 1. There is a precursor stage of very short duration at the electron transit time $\Delta t_1 \sim \tau_{tr}^e \equiv L_B / v_{th0}$ with $v_{th0} \equiv \sqrt{T_0 / m_e}$ the initial electron thermal speed, which follows the same scaling as in Eq. (3). Interestingly it produces rather limited cooling of the core plasma, $T_1 \geq 0.6T_0 \gg T_w$. The core plasma cooling is primarily accomplished in the next collisionless stage from $T_1 (\sim T_0)$ to $T_2 (\ll T_0)$, with $\Delta t_2 \gg \Delta t_1$. There is a transition stage $\Delta t_3 (\sim \Delta t_2)$ that connects the collisionless cooling phase to the eventual collisional cooling phase, in which Δt_4 is far longer than the main collisionless cooling stage of Δt_2 . The *most surprising and impactful finding* is that the main collisionless cooling phase from $T_1 \sim T_0$ to $T_2 \ll T_0$, is dominated by convective energy transport as opposed to the commonly accepted much faster electron parallel thermal conduction, e.g., Eq. (2). This yields a thermal quench time Δt_2 that scales with the ion transit time $\Delta t_2 \propto \tau_{tr}^i \equiv L_B / c_s$ with $c_s \equiv \sqrt{3(1+Z)T_0 / m_i}$ the ion sound speed (Z is the ion charge). The main thermal quench time of Δt_2 is thus *qualitatively different* from that of τ_{TQ} in Eq. (3), which constitutes

the prevailing textbook description of thermal loss by electron free-streaming along magnetic field lines.

The rest of the paper is organized as follows. In Section II, we explain the setup of the first-principles kinetic simulations. The simulation results are analyzed in Section III, where the physics underlying the four distinct phases of plasma cooling is elucidated with theory and modeling. The paper is concluded with a summary of results and additional discussions for current and planned tokamak experiments in Section IV. There is also an Appendix A that gives the derivation of the collisional cooling scaling.

II. METHODS

Simulation setup: We deployed first-principles kinetic simulations using the VPIC code [22] to investigate the cooling dynamics of an open field line plasma. The simulation domain is 1-D with domain size of $1400\lambda_{De}$, where λ_{De} is the Debye length for the initial plasma conditions with uniform electron and ion density $n_0 = 1 \times 10^{19} \text{cm}^{-3}$ and temperature $T_0 = 10 \text{keV}$. We use cell size $\Delta x = 0.1\lambda_{De}$ with 1000 electrons and 1000 hydrogen ions per cell. The time step $\Delta t = 1.357 \times 10^{-2} \omega_{pe}^{-1}$ is chosen according to the Courant condition. To elucidate the underlying physics, we perform two contrasting simulations with (1) thermobath boundary condition that models the cooling effect of a radiative cooling mass, and (2) an absorbing boundary. The thermobath boundary recycles particles by re-injecting electron-ion pairs with a clamped temperature $T_w = 0.01T_0$, while the absorbing boundary will absorb all the particles hitting the boundary.

III. FOUR DISTINCT PHASES OF PLASMA COOLING

Precursor phase ($T_{e\parallel}$ from T_0 to T_1 and $\Delta t_1 \sim \tau_{tr}^e$): At the onset of a plasma thermal quench when the hot plasma on the open field lines suddenly intercepts a cold boundary, $T_{e\parallel}(x=0, t)$ barely changes over a period that is approximately one third of τ_{tr}^e . This is simply the time for the so-called pre-cooling front (PF), which is driven by suprathermal electron loss and propagates from the boundary toward the core plasma at a speed $U_{PF} = 2.4v_{th0}$, to arrive at the plasma center ($x=0$). [23] This instance is marked by the black dashed vertical line in Fig. 2. The subsequent cooling of $T_{e\parallel}(x=0)$ is indeed driven by the electron conduction flux that follows a similar scaling as the flux limiting form in Eq. (2). Notice that for a nearly collisionless plasma, the conduction flux corresponding to $T_{e\parallel}$ cooling is given by $q_{en} \equiv \int m_e \tilde{v}_{\parallel}^3 f_e d^3\mathbf{v}$. Consequently, the duration of this phase does follow the free-streaming scaling previously given in Eq. (3). Remarkably the precursor phase ends abruptly when the so-called precooling trailing front (PTF) reaches the center. This is a second electron front that propagates from the boundary toward the core plasma, with a speed $U_{PTF} = \sqrt{2e\Delta\Phi_{RF}/m_e}$. [23] Here the reflecting potential $\Delta\Phi_{RF}$ is the result of the ambipolar electric field in the ion recession layer where a plasma rarefaction wave is formed. Since the ambipolar potential scales with

$T_{e\parallel}$, we would normally have $v_{th,e} < U_{PTF} < U_{PF}$, and thus $\Delta t_1 \sim \tau_{ir}^e$. The short duration of the precursor phase produces very limited cooling and typically $T_1 \geq 0.6T_0$.

Cooling flow phase ($T_{e\parallel}$ from T_1 to T_2 with $T_w < T_2 \ll T_0$ and $\Delta t_2 \sim \tau_{ir}^i$): Once the precooling trailing fronts reach the plasma center from both ends, q_{en} undergoes a qualitative transition from scaling with $v_{th,e}$ (i.e. $q_{en} \propto n_e v_{th,e} T_{e\parallel}$) to scaling with $V_{i\parallel}$ (i.e. $q_{en} \propto n_e V_{i\parallel} T_{e\parallel}$). Here $V_{i\parallel}$ is the parallel ion convective flow and ambipolar transport implies the parallel electron flow $V_{e\parallel} \approx V_{i\parallel}$. Previously we have shown that in a semi-infinite plasma bounded at one side only by a thermobath boundary, q_{en} always has the free-streaming flux-limiting form $n_e v_{th,e} T_{e\parallel}$ due to the cold electrons being pulled into the hot plasma by the ambipolar electric field. [23] The qualitative change of q_{en} in a bounded plasma is driven by how $T_{e\parallel}$ is being cooled in a long mean-free-path plasma where electron trapping is provided by the reflecting (ambipolar) potential along the magnetic field line on both ends.

The core cooling physics is most straightforwardly understood in a plasma with perfectly absorbing boundaries. Since the trapped-passing boundary is given by $v_c \equiv \sqrt{e\Delta\Phi_{RF}/m_e}$, and the truncated electron distribution at $x = 0$ has the form

$$f_0 = \frac{n_0}{(2\pi)^{3/2} v_{th0}^3} e^{-(v_{\parallel}^2 + v_{\perp}^2)/2v_{th0}^2} \Theta\left(1 - \frac{v_{\parallel}}{v_c}\right) \Theta\left(1 + \frac{v_{\parallel}}{v_c}\right),$$

with $\Theta(x)$ the Heaviside function satisfying $\Theta(x < 0) = 0$ and $\Theta(x > 0) = 1$. One can see that the parallel electron temperature $T_{e\parallel}(v_c, T_0) = \int m_e v_{\parallel}^2 f_e d^3\mathbf{v} / \int f_e d^3\mathbf{v} = (v_c^2/3v_{th0}^2) T_0$ of the electrostatically trapped long mean-free-path electrons cools drastically with a decreasing $v_c/v_{th0} \ll 1$. This correlates with a reducing reflecting potential $\Delta\Phi_{RF}$. Away from the symmetry point at $x = 0$, a finite parallel electron conduction flux arises from the asymmetric truncations (V_L and V_R) on the positive and negative sides of electron distribution in v_{\parallel}

$$f_e = \frac{n_0}{(2\pi)^{3/2} v_{th0}^3} e^{-(v_{\parallel}^2 + v_{\perp}^2)/2v_{th0}^2} \Theta\left(1 - \frac{v_{\parallel}}{V_R}\right) \Theta\left(1 + \frac{v_{\parallel}}{V_L}\right).$$

In the limit of significant plasma cooling, one can write $V_{e\parallel} \approx (-V_L + V_R)/2$ and find a convective energy flux scaling for electron thermal conduction

$$q_{en} \approx \frac{6T_{e\parallel}}{5T_0} n_e V_{e\parallel} T_{e\parallel}. \quad (4)$$

In a cooling plasma of $T_{e\parallel} \ll T_0$, one recovers the remarkable result of $q_{en} \ll n_e V_{e\parallel} T_{e\parallel}$ observed in VPIC simulations.

An even more interesting and impactful result is on q_{en} of a plasma with thermobath boundary conditions. The subtlety is that cold electrons from the boundary plasmas can follow the ambipolar electric field into the core plasma. This cold electron beam component was previously found to restore the free-streaming flux-limiting form of Eq. (2) in a semi-infinite plasma [23]. With cold boundary plasmas on both ends at $x = \pm L_B$, the cold electron beams from both sides, accelerated by the ambipolar electric field, nearly cancel each other, in the electron flow and thermal conduction flux. As the result, q_{en} takes on the *qualitatively different result by retaining the convective energy transport scaling* in the absorbing wall case.

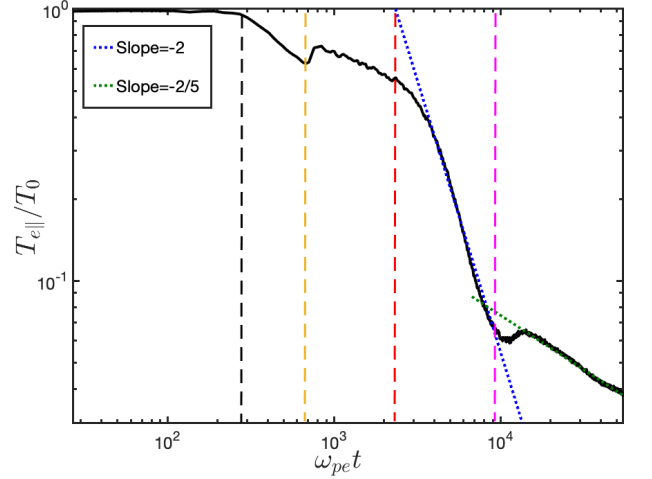


FIG. 2: $T_{e\parallel}(x = 0, t)$ of a slab ($x \in [-L_B, L_B]$) is shown for a VPIC simulation with $L_B = 1400\lambda_{De}$ (λ_{De} the electron Debye length), an initially uniform plasma of $m_e/m_i = 1/100$, $Z = 1$ and $K_{n,0} = 37$. Thermobath boundary on two ends has $T_w = 0.01T_0$. The vertical dashed lines mark the moments when the four fronts reach the center, while the dotted lines with slopes of -2 (blue) and $-2/5$ (green) are marked for the cooling flow phase (Δt_2) and collisional phase (Δt_4).

Quantitatively, once the ion recession front, which propagates from the boundary to the plasma center at the local ion sound speed, reaches the center, q_{en} has settled into a magnitude that is solidly *sub-dominant* to the actual convective energy flux $3n_e V_{i\parallel} T_{e\parallel}$, as shown by the black lines in Fig. 3(e).

Remarkably the core plasma cooling history in the cooling flow phase is similar if not nearly identical between the absorbing and thermobath boundary cases. This is connected to thermal conduction being sub-dominant to convective energy transport in both cases. Next, we use the absorbing wall case to illustrate the characteristics of the cooling history. An important result from the VPIC simulations is that the cooling flow $V_{i\parallel}$ linearly grows in x from zero at $x = 0$ to the Bohm speed u_{Bohm} near $x = L_B$, and it decays in time due to plasma cooling. This can be understood via a separable solution $V_{i\parallel}(x, t) = P(x)Q(t)$ to the ion momentum equation, where the decay of the plasma flow is mostly balanced by the inertial term (e.g., see Fig. 3),

$$\frac{\partial}{\partial t} V_{i\parallel} + V_{i\parallel} \frac{\partial}{\partial x} V_{i\parallel} = -\nabla p \approx 0. \quad (5)$$

The separable solution has

$$\frac{dP}{dx} = -\frac{dQ/dt}{Q^2} = C_0, \quad (6)$$

with C_0 a constant. The solution $P(x) = C_0 x$ underlies the aforementioned VPIC simulation result. In the normal situation with an upstream Maxwellian plasma, $u_{Bohm} \approx \sqrt{(ZT_{e\parallel} + 3T_{i\parallel})/m_i}$ because of the parallel heat flux into the sheath [24, 25]. While for the nearly collisionless plasma in the cooling flow phase during a thermal quench, the thermal

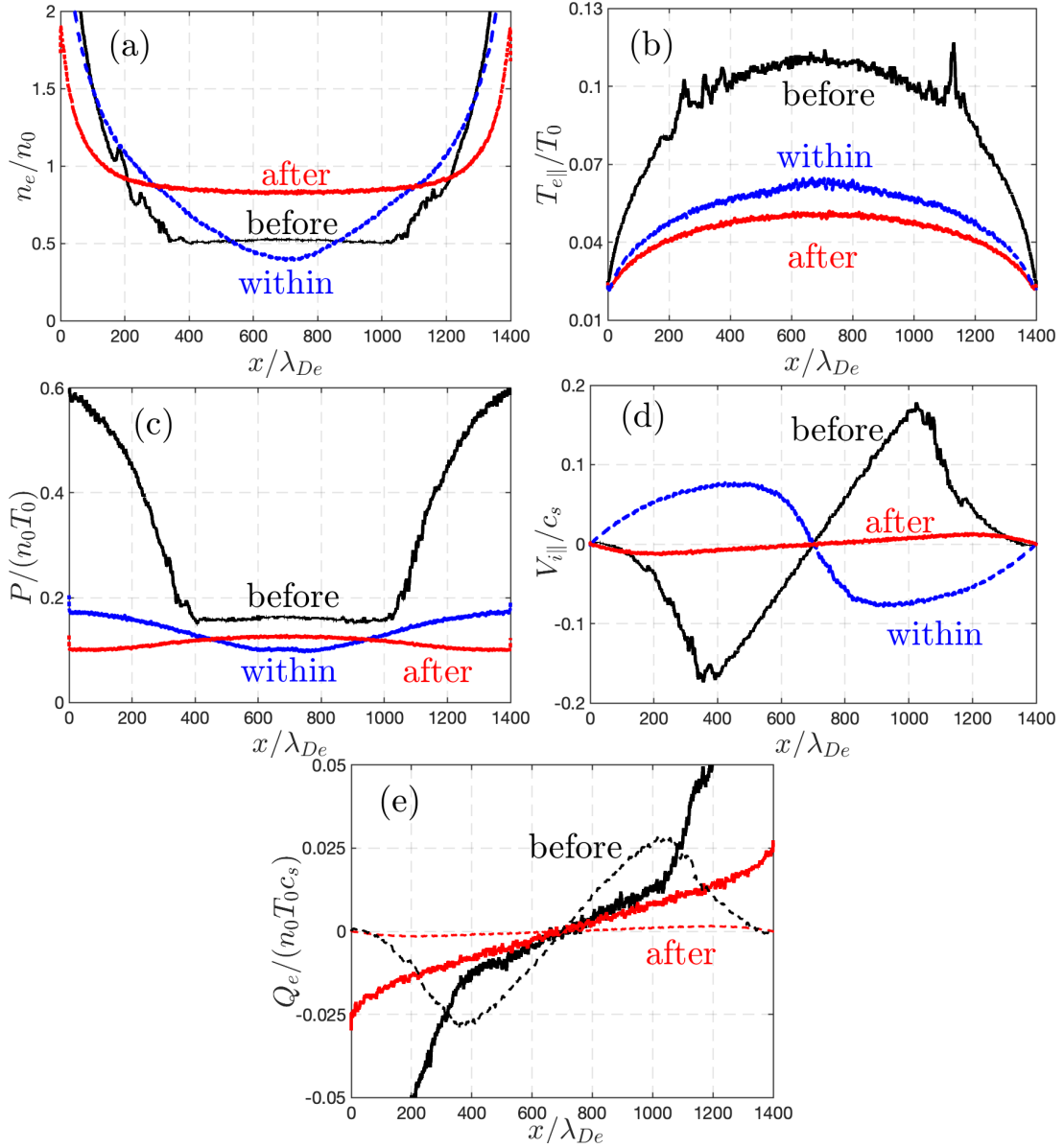


FIG. 3: Spatial profiles of (a) n_e , (b) $T_{e\parallel}$, (c) $P = n_e T_{e\parallel} + n_i T_{i\parallel}$ and (d) $V_{i\parallel}$ before (inside the cooling flow phase), within, and after the transition phase from the simulation in Fig. 2. (e) shows the profile of electron thermal conduction (solid thicker lines) and convection ($3n_e V_{i\parallel} T_{e\parallel}$, dash thinner lines) fluxes (Q_e) before and after the transition phase. Before and after the transition, the thermal conduction is q_{en} and $q_{e\parallel}$ defined in Eq. (4) and Eq. (1), respectively.

conduction is insignificant, so $u_{Bohm} \approx \sqrt{(3ZT_{e\parallel} + 3T_{i\parallel})/m_i}$. Since the cooling starts at T_0 , the Bohm speed at $t = 0$ is simply the parallel sound speed $c_s \equiv \sqrt{3(Z+1)T_0/m_i}$ in a magnetized plasma with strong temperature anisotropy, so we can write $C_0 = c_s/L_B$, which introduces an ion transit time $\tau_{ir}^i = L_B/c_s$ for Q ,

$$Q = \left(\delta + \frac{t}{\tau_{ir}^i} \right)^{-1}. \quad (7)$$

Here $\delta \sim 1$ depends on the condition when $T_{e\parallel}$ becomes uniform and we assumed $T_{i\parallel} \approx T_{e\parallel}$ due to the convective heat flux dominating the cooling. Similarly a separable solution

$T_{e\parallel} = M(x)N(t)$ can be found from the electron energy equation, [26]

$$n_e \frac{\partial}{\partial t} T_{e\parallel} + n_e V_{e\parallel} \frac{\partial}{\partial x} T_{e\parallel} + 2n_e T_{e\parallel} \frac{\partial}{\partial x} V_{e\parallel} + \frac{\partial}{\partial x} q_{e\parallel} = 0. \quad (8)$$

Ignoring the sub-dominant $\partial q_{en}/\partial x$ term and the $n_e V_{e\parallel} \partial T_{e\parallel}/\partial x$ term because of weak $T_{e\parallel}$ variation, one finds $d \ln N(t)/dt = -2C_0 Q(t)$ for

$$\frac{T_{e\parallel}(t)}{T_0} = N(t) = \left(\delta + \frac{t}{\tau_{ir}^i} \right)^{-2}, \quad (9)$$

with $M(x) \approx T_0$. This reveals two pieces of interesting and

important physics: (1) the characterized time of collisionless core $T_{e\parallel}$ cooling is given by the ion sound transit time $\Delta t_2 \sim \tau_{ir}^i$; and (2) $T_{e\parallel}(t) \propto t^{-2}$ for $t/\tau_{ir}^i \gg 1$ as shown in Fig. 2. Substitution of Eq. (9) into u_{Bohm} gives $u_{Bohm} = P(x = L_B)Q$ as expected so that the solutions are self-consistent.

The temperature T_2 signifies the beginning of a transition from collisionless to collisional cooling, and it is set by the constraint that the convection flux equals the Braginskii conduction, which suggests a Knudsen number at the transition

$$K_{n,2} \sim c_s/v_{th,e} \sim \sqrt{m_e(1+Z)/m_i}. \quad (10)$$

If we ignore the small density variation at the core (see Fig. 3) so that $K_{n,2} \approx K_{n,0}(T_2/T_0)^2$, we find

$$T_2 \sim T_0 K_{n,0}^{-1/2} [m_e(1+Z)/m_i]^{1/4}. \quad (11)$$

This agrees well with VPIC simulation data in Fig. 2, where $T_2 \approx 0.06T_0$ from Eq. (11) and the simulation. The cooling time from T_1 to T_2 is then found from Eq. (9) to be

$$\Delta t_2 \sim K_{n,0}^{1/4} [m_e(1+Z)/m_i]^{-1/8} \tau_{ir}^i. \quad (12)$$

For plasma parameters in Fig. 2, $\Delta t_2 \sim 4\tau_{ir}^i$, in good agreement with the simulation data.

Transition phase ($T_{e\parallel} \sim T_2 \sim T_3$ and $\Delta t_3 \sim \tau_{ir}^i$): The cooling flow meets its eventual collapse when the boundary plasma becomes over-pressured because of density build-up in the presence of decreasing temperature gradient. This sets off a recompression of the core that transiently heats the plasma temperature, especially that of the ions. Due to the strong Landau damping of ion-acoustic waves, the recompression flow is removed over one thermal ion transit period, so $\Delta t_3 \approx \tau_{ir}^i(T_2) \sim \Delta t_2$, leaving a core plasma temperature $T_3 \approx T_2$ at the end of the one-bounce transition period, as shown in Fig. 2.

Collisional cooling phase ($T_{e\parallel}$ from T_3 to T_w , and $\Delta t_4 \gg \tau_{ir}^i$): Collisional cooling is dominated by the thermal conduction $q_{e\parallel}$ given by Braginskii in Eq. (1):

$$3n_e \frac{\partial}{\partial t} T_{e\parallel} + \frac{\partial}{\partial x} q_{e\parallel} = 0. \quad (13)$$

A separable solution $T_{e\parallel} = M(x)N(t)$ with $M(x) \neq const.$ has the core $T_{e\parallel}$ evolve in time as

$$\frac{T_{e\parallel}}{T_3} = \left(\delta_2 + 1.6K_{n,3} \sqrt{\frac{T_3}{m_e}} \frac{t}{L_B} \right)^{-2/5}, \quad (14)$$

where $\delta_2 \sim 1$ accounts for Δt_2 and Δt_3 in t . Here all the variables are normalized using the quantities at the beginning of collisional TQ including the Knudsen number $K_{n,3}$. Therefore, this solution can be applied to plasma that is initially within the collisional regime. For an initially collisionless fusion plasma, we can substitute $T_3 \approx T_2$ and hence $K_{n,3} \approx K_{n,2}$ into Eq. (14) to obtain

$$\frac{T_{e\parallel}}{T_3} = \left\{ \delta_2 + 1.6K_{n,0}^{-1/4} \left[\frac{m_e(1+Z)}{m_i} \right]^{1/8} \frac{t}{\tau_{ir}^i} \right\}^{-2/5}. \quad (15)$$

Here t is naturally normalized by τ_{ir}^i as in Eq. (9) for the cooling flow phase. The factor in front has weak powers ($-1/4$ and $1/8$ respectively) of $K_{n,0}$ and $m_e(1+Z)/m_i$, so it is also a number of order unity, like that in Eq. (9). What is different is that $T_{e\parallel}(t) \propto t^{-2/5}$ as shown in Fig. 2, in sharp contrast to $T_{e\parallel}(t) \propto t^{-2}$ in the cooling flow phase. This explains a much slower core TQ in the collisional regime than that in the collisionless regime. Specifically, the core TQ from T_3 to T_w takes

$$\Delta t_4 \sim \left(\frac{T_w}{T_0} \right)^{-5/2} K_{n,0}^{-1} \left[\frac{m_e(1+Z)}{m_i} \right]^{1/2} \tau_{ir}^i. \quad (16)$$

It is easy to check that $\Delta t_4 \gg \Delta t_2$ for $T_w \ll T_2$.

IV. CONCLUSION AND DISCUSSION

In conclusion, the main core thermal collapse ($T_0 \rightarrow T_2 \ll T_0$) is mostly accomplished in the cooling flow phase with the duration that is a few times the ion sound transit time $\Delta t_2 \sim L_B/c_s$, due to the surprising physics that electron thermal conduction is sub-dominant to convective energy transport in a nearly collisionless cooling plasma. This is followed by a transition phase in which over-pressured boundary plasma reheats the core plasma by compression. The final collisional cooling phase takes so long that the experimentally observed deep cooling to tens or a few eVs in milliseconds or shorter time must be due to a different mechanism, with impurity radiation a leading candidate. The source of these impurities, in naturally occurring disruptions, is likely the result of intense plasma-material interaction in the cooling phases preceding the final collisional stage, during which the outgoing plasma power flux is far greater.

The physics scaling reveals that for a fusion-grade plasma in which T_0 and n_0 are severely constrained, the variability in TQ duration, which experimentally is associated with Δt_2 , is mostly set by the magnetic connection length L_B . This potentially provides a means to determine the otherwise difficult-to-access L_B of globally stochastic magnetic fields. To quantify our findings, we show $\Delta t_{2,4}$ from Eqs. (12,16) and T_2 from Eq. (11), of representative DIII-D and ITER plasmas for a range of L_B in Fig. 4. This provides a baseline prediction of TQ duration for comparison with experimental measurements and more involved transport calculations. For all cases considered, it is striking that the duration of the collisional cooling phase, Δt_4 , is orders of magnitude longer than that of the collisionless cooling phase Δt_2 . Furthermore, for longer magnetic connection length L_B , the ratio of Δt_4 and Δt_2 becomes larger. The transition temperature T_2 that separates the collisionless and collisional cooling phases becomes lower if a stronger field line stochasticity produces a shorter magnetic connection length L_B .

Since the analysis given in this paper focuses on the regime of parallel transport dominating over perpendicular transport, the experimentally applicable regime for the predicted results of $\Delta t_{2,4}$ and T_2 is toward the end of short magnetic connection length L_B , for which $\Delta t_{2,4}$ and T_2 are of smaller values. For $L_B \sim 10^3$ m, parallel transport can certainly produce a

core temperature collapse on the order of a millisecond or so. The main thermal quench time (Δt_2) becomes shorter if the magnetic connection length is further reduced, reaching $\Delta t_2 < 0.1$ ms for $L_B \sim 10$ m. Such a short magnetic connection length can be experimentally realized by the injected high-Z pellets that directly intersect the core plasma, even with the nested flux surfaces remaining intact.

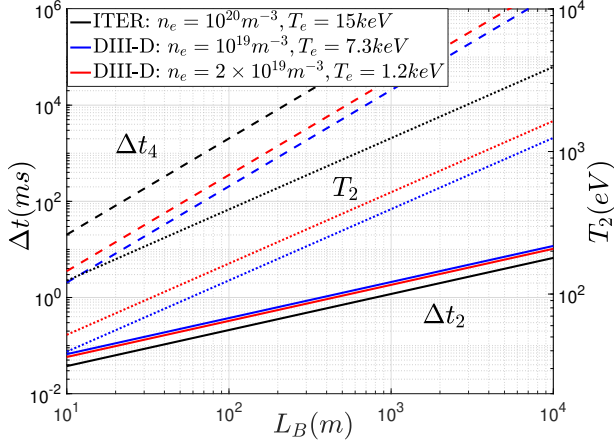


FIG. 4: $\Delta t_{2,4}$ from Eqs. (12,16) (solid and dash lines for left y-axis) and T_2 from Eq. (11) (dotted lines for right y-axis) of representative DIII-D and ITER plasmas. Here we choose hydrogen ions and $T_w = 10$ eV.

ACKNOWLEDGMENTS

We thank the U.S. Department of Energy Office of Fusion Energy Sciences and Office of Advanced Scientific Computing Research for support under the Tokamak Disruption Simulation (TDS) Scientific Discovery through Advanced Computing (SciDAC) project at Los Alamos National Laboratory (LANL) under contract No. 89233218CNA000001. Y.Z. was supported under a Director's Postdoctoral Fellowship at LANL. This research used resources of the National Energy Research Scientific Computing Center (NERSC), a U.S. Department of Energy Office of Science User Facility operated under Contract No. DE-AC02-05CH11231, and the Los Alamos National Laboratory Institutional Computing Program, which is supported by the U.S. Department of Energy National Nuclear Security Administration under Contract No. 89233218CNA000001.

Appendix A: Derivation of collisional cooling scaling in Eq. (14)

In a strong collisional plasma, only considering the thermal flux in the energy equation provides [20]

$$3n_e \frac{\partial T_e}{\partial t} = -\frac{\partial q_e}{\partial x} = \frac{\partial}{\partial x} (\kappa_{\parallel} \frac{\partial T_e}{\partial x}), \quad (\text{A1})$$

where

$$\kappa = 3.16 \frac{n_e T_e \tau_e}{m_e}, \quad (\text{A2})$$

and we ignored the subscript \parallel in T_e and κ . Note that we have summed up the energy equations of electrons and ions and kept only the electron thermal flux. It is also worth noting that $n_e \tau_e / T_e^{3/2}$ is a constant when ignoring the dependence of $\ln \Lambda$ on the density and temperature so that we obtain

$$\frac{\partial T_e}{\partial t} = \frac{3.16}{3} \frac{2}{7} \frac{\tau_e}{m_e T_e^{3/2}} \frac{\partial^2}{\partial x^2} T_e^{7/2}. \quad (\text{A3})$$

Now if we ignore the density variation in space and time, we arrive at the heat equation with a constant coefficient $C_0 \approx 0.3 \lambda_{emfp,3} v_{th,3} / T_3^{5/2}$, where $v_{th,3} = \sqrt{T_3 / m_e}$ and $\lambda_{emfp,3}$ are the electron thermal speed and mean free path at the temperature T_3 (note that T_3 is used for the normalization of the electron temperature).

A separable solution $T_e = M(x)N(t)$ would yield

$$\frac{dN/dt}{C_0 N^{7/2}} = \frac{1}{M} \frac{\partial^2 M^{7/2}}{\partial x^2} = \text{const.} \equiv C_1 < 0, \quad (\text{A4})$$

from which we obtain

$$N = \left(N_0^{-5/2} - 2.5 C_0 C_1 t \right)^{-2/5}, \quad (\text{A5})$$

where $N_0 = N(t=0)$. For the equation of $M(x)$, we define $\Upsilon = M^{7/2}$, which satisfies

$$\frac{\partial^2 \Upsilon}{\partial x^2} = C_1 \Upsilon^{2/7}. \quad (\text{A6})$$

Such an equation has a solution of the implicit form

$$\frac{H(C_1, C_2, \Upsilon)^2 \Upsilon^2}{C_2} = (x + C_3)^2 \quad (\text{A7})$$

where C_2 and C_3 are constants, and

$$H(C_1, C_2, \Upsilon) = {}_2F_1 \left(\frac{1}{2}, \frac{7}{9}, \frac{16}{9}, -\frac{14C_1 \Upsilon^{9/7}}{9C_2} \right). \quad (\text{A8})$$

is a hypergeometric function [27].

Now we consider the boundary conditions to settle down $C_{1,2,3}$, where we let N be dimensionless such that $M(x=0) = T_3$ at the center of the simulation domain. As a result, $\Upsilon(x=0) = M(x=0)^{7/2} = T_3^{7/2}$. We assume that the wall temperature is negligibly small $T_w \approx 0$ so that $\Upsilon(x=L_B) = 0$. These conditions turn into

$$C_3 = -L_B, \quad (\text{A9})$$

$$H \left(C_1, C_2, T_3^{7/2} \right)^2 T_3^7 = C_2 L_B^2. \quad (\text{A10})$$

To solve C_1 and C_2 from Eq. (A10), we need more conditions, which are $\frac{dM}{dx}|_{x \rightarrow 0} \rightarrow 0$ due to the system symmetry and $\frac{dM}{dx} <$

0 at $x > 0$. Recalling $C_1 < 0$, these conditions together with Eq. (A10) provide $C_1 \rightarrow -2.13T_3^{5/2}/L_B^2$ and $C_2 = 3.31T_3^7/L_B^2$.

As a result, Eq. (A5) becomes

$$\frac{T_e}{T_3} = \left(N_0^{-5/2} + 1.6v_{th,3} \frac{\lambda_{emfp,3}}{L_B} \frac{t}{L_B} \right)^{-2/5} \quad (\text{A11})$$

which is Eq. (14) in the main text.

-
- [1] E. Doyle, W. Houlberg, Y. Kamada, V. Mukhovatov, T. Osborne, A. Polevoi, G. Bateman, J. Connor, J. C. (retired), T. Fujita, X. Garbet, T. Hahm, L. Horton, A. Hubbard, F. Imbeaux, F. Jenko, J. Kinsey, Y. Kishimoto, J. Li, T. Luce, Y. Martin, M. Ossipenko, V. Parail, A. Peeters, T. Rhodes, J. Rice, C. Roach, V. Rozhansky, F. Ryter, G. Saibene, R. Sartori, A. Sips, J. Snipes, M. Sugihara, E. Synakowski, H. Takenaga, T. Takizuka, K. Thomsen, M. Wade, H. Wilson, I. T. P. T. Group, I. C. Database, M. Group, I. Pedestal, and E. T. Group, Chapter 2: Plasma confinement and transport, *Nuclear Fusion* **47**, S18 (2007).
- [2] A. H. Boozer, Physics of magnetically confined plasmas, *Rev. Mod. Phys.* **76**, 1071 (2004).
- [3] T. Hender, J. Wesley, J. Bialek, A. Bondeson, A. Boozer, R. Buttery, A. Garofalo, T. Goodman, R. Granetz, Y. Gribov, O. Gruber, M. Gryaznevich, G. Giruzzi, S. Günter, N. Hayashi, P. Helander, C. Hegna, D. Howell, D. Humphreys, G. Huysmans, A. Hyatt, A. Isayama, S. Jardin, Y. Kawano, A. Kellman, C. Kessel, H. Koslowski, R. L. Haye, E. Lazzaro, Y. Liu, V. Lukash, J. Manickam, S. Medvedev, V. Mertens, S. Mirnov, Y. Nakamura, G. Navratil, M. Okabayashi, T. Ozeki, R. Paccagnella, G. Pautasso, F. Porcelli, V. Pustovitov, V. Riccardo, M. Sato, O. Sauter, M. Schaffer, M. Shimada, P. Sonato, E. Strait, M. Sugihara, M. Takechi, A. Turnbull, E. Westerhof, D. Whyte, R. Yoshino, H. Zohm, D. the ITPA MHD, and M. C. T. Group, Chapter 3: Mhd stability, operational limits and disruptions, *Nuclear Fusion* **47**, S128 (2007).
- [4] V. Riccardo, A. Loarte, *et al.*, Timescale and magnitude of plasma thermal energy loss before and during disruptions in JET, *Nuclear fusion* **45**, 1427 (2005).
- [5] I. P. E. G. on Disrup MHD and I. P. B. Editors, Chapter 3: MHD stability, operational limits and disruptions, *Nuclear Fusion* **39**, 2251 (1999).
- [6] M. Shimada, D. Campbell, V. Mukhovatov, M. Fujiwara, N. Kimeva, K. Lackner, M. Nagami, V. Pustovitov, N. Uckan, J. Wesley, *et al.*, Chapter 1: Overview and summary, *Nuclear Fusion* **47**, S1 (2007).
- [7] A. Nedospasov, Thermal quench in tokamaks, *Nuclear fusion* **48**, 032002 (2008).
- [8] A. Bondeson, R. Parker, M. Hugon, and P. Smeulders, MHD modelling of density limit disruptions in tokamaks, *Nuclear Fusion* **31**, 1695 (1991).
- [9] V. Riccardo, P. Andrew, L. Ingesson, and G. Maddaluno, Disruption heat loads on the JET MkiIGB divertor, *Plasma Physics and Controlled Fusion* **44**, 905 (2002).
- [10] E. Nardon, A. Fil, M. Hoelzl, G. Huijsmans, *et al.*, Progress in understanding disruptions triggered by massive gas injection via 3D non-linear MHD modelling with JOREK, *Plasma Physics and Controlled Fusion* **59**, 014006 (2016).
- [11] R. Sweeney, W. Choi, M. Austin, M. Brookman, V. Izzo, M. Knolker, R. La Haye, A. Leonard, E. Strait, F. Volpe, *et al.*, Relationship between locked modes and thermal quenches in DIII-D, *Nuclear Fusion* **58**, 056022 (2018).
- [12] G. Federici, P. Andrew, P. Barabaschi, J. Brooks, R. Doerner, A. Geier, A. Herrmann, G. Janeschitz, K. Krieger, A. Kukushkin, *et al.*, Key ITER plasma edge and plasma-material interaction issues, *Journal of Nuclear Materials* **313**, 11 (2003).
- [13] S. K. Combs, S. J. Meitner, L. R. Baylor, J. B. Caughman, N. Commaux, D. T. Fehling, C. R. Foust, T. C. Jernigan, J. M. McGill, P. B. Parks, *et al.*, Alternative techniques for injecting massive quantities of gas for plasma-disruption mitigation, *IEEE transactions on plasma science* **38**, 400 (2010).
- [14] N. Commaux, D. Shiraki, L. R. Baylor, E. Hollmann, N. Eidietis, C. Lasnier, R. Moyer, T. Jernigan, S. Meitner, S. K. Combs, *et al.*, First demonstration of rapid shutdown using neon shattered pellet injection for thermal quench mitigation on dIII-d, *Nuclear Fusion* **56**, 046007 (2016).
- [15] C. Paz-Soldan, P. Aleynikov, E. Hollmann, A. Lvovskiy, I. Bykov, X. Du, N. Eidietis, and D. Shiraki, Runaway electron seed formation at reactor-relevant temperature, *Nuclear Fusion* **60**, 056020 (2020).
- [16] D. Gray and J. Kilkenny, The measurement of ion acoustic turbulence and reduced thermal conductivity caused by a large temperature gradient in a laser heated plasma, *Plasma Physics* **22**, 81 (1980).
- [17] A. R. Bell, Non-spitzer heat flow in a steadily ablating laser-produced plasma, *The Physics of Fluids* **28**, 2007 (1985), <https://aip.scitation.org/doi/pdf/10.1063/1.865378>.
- [18] D. Shvarts, J. Delettrez, R. McCrory, and C. Verdon, Self-consistent reduction of the spitzer-härm electron thermal heat flux in steep temperature gradients in laser-produced plasmas, *Physical Review Letters* **47**, 247 (1981).
- [19] S. Landi and F. Pantellini, On the temperature profile and heat flux in the solar corona: Kinetic simulations, *Astronomy & Astrophysics* **372**, 686 (2001).
- [20] S. I. Braginskii, *Reviews of Plasma Physics*, ed. M. A. Leontovich, Vol.1, pp. 205-311 (Consultants Bureau, New York, 1965).
- [21] S. Atzeni and J. Meyer-Ter-Vehn, *The physics of inertial fusion* (Oxford University Press, Inc., 2004).
- [22] K. J. Bowers, B. Albright, L. Yin, B. Bergen, and T. Kwan, Ultrahigh performance three-dimensional electromagnetic relativistic kinetic plasma simulation, *Physics of Plasmas* **15**, 055703 (2008).
- [23] Y. Zhang, J. Li, and X.-Z. Tang, Cooling flow regime of plasma thermal quench, <https://arxiv.org/abs/2207.09974> (2022).
- [24] X.-Z. Tang and Z. Guo, Critical role of electron heat flux on bohm criterion, *Physics of Plasmas* **23**, 120701 (2016).
- [25] Y. Li, B. Srinivasan, Y. Zhang, and X.-Z. Tang, Bohm criterion of plasma sheaths away from asymptotic limits, *Phys. Rev. Lett.* **128**, 085002 (2022).
- [26] Z. Guo and X.-Z. Tang, Parallel transport of long mean-free-path plasmas along open magnetic field lines: Plasma profile variation, *Physics of Plasmas* **19**, 082310 (2012).
- [27] Y. A. Brychkov, *Handbook of Special Functions: Derivatives*,

Integrals, Series and Other Formulas (1st ed.) (Chapman and

Hall/CRC., New York, 2008).